Original Article

MOLECULAR METABOLISM

Conditional hepatocyte ablation of PDIA1 uncovers indispensable roles in both APOB and MTTP folding to support VLDL secretion

Zhouji Chen[1,], Shiyu Wang[1,4], Anita Pottekat[1], Alec Duffey[1], Insook Jang[1], Benny H. Chang[2], Jaehyung Cho[3], Brian N. Finck[3], Nicholas O. Davidson[3], Randal J. Kaufman[1,*]**

ABSTRACT

Objectives: The assembly and secretion of hepatic very low-density lipoprotein (VLDL) plays pivotal roles in hepatic and plasma lipid homeostasis. Protein disulfide isomerase A1 (PDIA1/*P4HB*) is a molecular chaperone whose functions are essential for protein folding in the endoplasmic reticulum. Here we investigated the physiological requirement *in vivo* for PDIA1 in maintaining VLDL assembly and secretion.
Methods: *Pdia1/P4hb* was conditionally deleted in adult mouse hepatocytes and the phenotypes characterized. Mechanistic analyses in primary hepatocytes determined how PDIA1 ablation alters MTTP synthesis and degradation as well as altering synthesis and secretion of Apolipoprotein B (APOB), along with complementary expression of intact PDIA1 vs a catalytically inactivated PDIA1 mutant.
Results: Hepatocyte-specific deletion of *Pdia1/P4hb* inhibited hepatic MTTP expression and dramatically reduced VLDL production, leading to severe hepatic steatosis and hypolipidemia. *Pdia1*-deletion did not affect mRNA expression or protein stability of MTTP but rather prevented *Mttp* mRNA translation. We demonstrate an essential role for PDIA1 in MTTP synthesis and function and show that PDIA1 interacts with APOB in an MTTP-independent manner via its molecular chaperone function to support APOB folding and secretion.
Conclusions: PDIA1 plays indispensable roles in APOB folding, MTTP synthesis and activity to support VLDL assembly. Thus, like APOB and MTTP, PDIA1 is an obligatory component of hepatic VLDL production.

Keywords Fatty liver disease; Protein disulfide isomerase A1; Microsomal triglyceride transfer protein; Protein folding; Unfolded protein response; VLDL secretion; Lipoprotein metabolism

1. INTRODUCTION

Disturbances in hepatic and plasma lipid metabolism are common feature of metabolic syndrome, which can directly increase the risk for liver and/or cardiovascular diseases associated with the rapidly increasing obesity pandemic in the modern world [1–4]. Cellular processes involving the biosynthesis and secretion of hepatic very low-density lipoprotein (VLDL) play a pivotal role in the regulation of hepatic and plasma lipid homeostasis because VLDL production is the sole mechanism for the liver to export triglyceride (TG) to the extrahepatic tissues for utilization or storage. Overproduction of hepatic VLDL is a common cause of hyperlipidemia in obesity and type II diabetes [2,4–7]. On the contrary, genetic defects in hepatic VLDL assembly and secretion cause metabolic dysfunction associated steatotic liver disease (MASLD) in mice and humans [6,8–14]. Recent clinical studies suggest that reduced hepatic VLDL secretion also contributes to MASLD progression to steatohepatitis (MASH) in obese subjects [15,16]. Thus, identifying novel factors governing VLDL assembly and secretion remains an important focus of intensive investigation [13,17–26].

The biosynthesis of VLDL is generally believed to follow a two-step process occurring in the lumen of the endoplasmic reticulum (ER) [6,7,14]. The initial step involves the translocation of the nascent apolipoprotein B (APOB) polypeptide across the ER membrane and co-translational lipidation of APOB by the microsomal TG transfer protein (MTTP), leading to the formation of a primordial APOB particle [6,14,27]. The second step involves the bulk addition of TG to VLDL and chylomicron precursors in the smooth ER [6,7,14,28] and to a lesser extent in the Golgi apparatus [6,29,30], through the fusion of pre-VLDL/chylomicron particles with luminal lipid droplets in these secretory compartments. The maturation of VLDL particles highly depends on the availability of TG in secretory compartments,

[1]Degenerative Diseases Program, Center for Genetics and Aging Research, Sanford Burnham Prebys Medical Discovery Institute, 10901 N. Torrey Pines Rd, La Jolla CA 92037, USA [2]Section of Nephrology, Division of Internal Medicine, The University of Texas MD Anderson Cancer Center, Houston, TX, USA [3]Department of Medicine, Washington University School of Medicine, St. Louis, Missouri, USA

[4] Present address for S.W.: Sanegene Bio, Fl. 14th, 1 Broadway, Cambridge, MA 02142, USA.

*Corresponding author. E-mail: rkaufman@sbpdiscovery.org (R.J. Kaufman).

**Corresponding author. E-mail: zchen@sbpdiscovery.org (Z. Chen).

Received December 8, 2023 • Revision received January 4, 2024 • Accepted January 6, 2024 • Available online 9 January 2024

https://doi.org/10.1016/j.molmet.2024.101874

especially the smooth ER [6,7,31]. APOB is an obligatory structural component of the VLDL particle without which TG-rich lipoproteins cannot be formed [6,12,22,32]. The human liver synthesizes only full-length APOB (APOB100) whereas mammalian intestinal enterocytes produce a shorter isoform APOB48 (the N-terminal 48 % of APOB100) through RNA editing which modifies *Apob* mRNA at codon 2153, converting a glutamine (CAA) codon to a (UAA) stop codon [14,33,34]. Unlike human liver, which synthesizes only APOB100, murine liver expresses APOBEC1 and synthesizes both APOB100 and APOB48 following *Apob* mRNA editing [14,33,35,36]. APOB is constitutively expressed in the liver but is subjected to intracellular degradation depending on the availability of neutral lipids for assembly and secretion [6,14,22,37].

MTTP is an ER-resident heterodimer consisting of a unique large 97 kDa α-subunit (encoded by *MTTP*) and the multifunctional protein disulfide isomerase A1 (PDIA1) β-subunit (55 kDa, encoded by *P4HB*) [6,7,14,38,39]. MTTP co-localizes with APOB in a tissue-specific manner mainly in the liver and intestines [6,7]. Like APOB, MTTP is absolutely required for the biogenesis of VLDL by the liver and chylomicrons by the small intestine [7,14,33,38]. Mutations in MTTP cause defective or missing MTTP function, resulting in abetalipoproteinemia, a rare autosomal recessive disorder in which APOB-containing lipoproteins are absent in the plasma due to defective VLDL and chylomicron assembly [14,38,39]. Deletion of *Mttp* in liver [40] or small intestine [41,42] in mice also abolishes VLDL and chylomicron assembly and secretion, respectively. In the absence of MTTP function, the nascent APOB polypeptide, especially ApoB100, is rapidly degraded by proteasome-mediated proteolysis [7,37,40,43], whereas APOB48 may escape intracellular degradation and is secreted as lipid-poor APOB48-particles [14,40,42,43]. Those findings are consistent with earlier studies that show MTTP inhibitors preferentially promote APOB100 degradation [44].

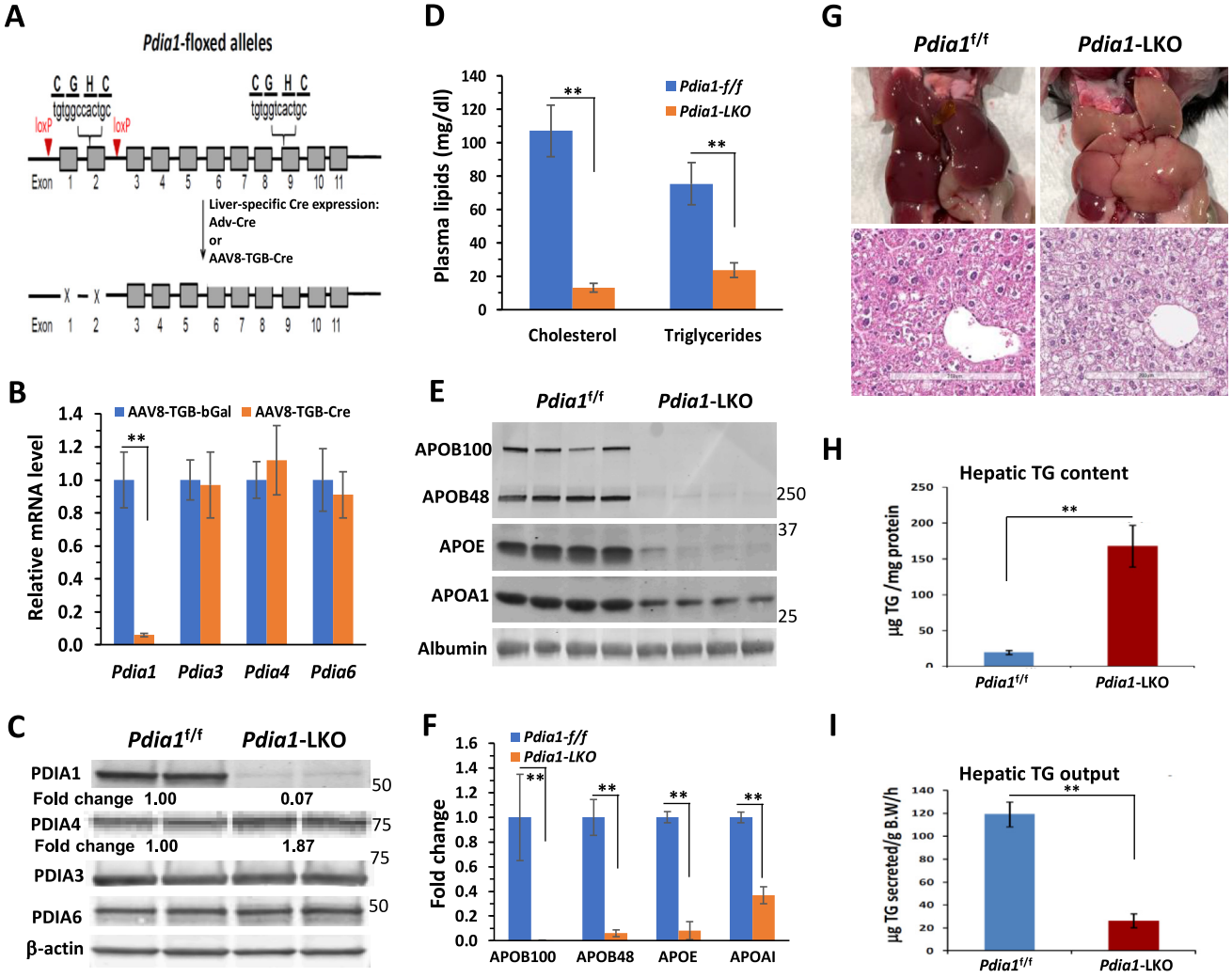

Figure 1: Hepatocyte-specific *Pdia1* deletion induces severe hypolipidemia and hepatic steatosis with a blockade of hepatic TG export. A. Schematic shows floxed exons 1 and 2 of the *Pdia1* allele (*Pdia1*$^{f/f}$). Generation of hepatocyte-specific PDIA1-ablated mice (*Pdia1*-LKO) was produced using Ad-CMV-Cre or AAV8-TBG-Cre. **B.** Transduction of *Pdia1*$^{f/f}$ with AAV8-TBG-Cre eliminated *Pida1* mRNA in the liver but did not affect the mRNA levels of other PDI protein family members. **C.** PDIA1 was absent in the livers of *Pdia1*-LKO accompanied with upregulation of PDIA4. **D.** Plasma levels of total cholesterol and TG were both greatly reduced in *Pdia1*-LKO mice (n = 5). **E** and **F.** APOB100, APOB48 and APOE were nearly absent in plasma of *Pdia1*-LKO mice, with a reduced level of ApoA1 but plasma albumin levels were not changed. Each lane represents a sample from individual mouse. **G.** Liver images and H/E-stained liver sections demonstrate severe liver fat accumulation in *Pdia1*-LKO mice. Scale bar: 200 μm. **H.** Hepatic TG content was markedly increased in *Pdia1*-LKO mice (n = 5). **I.** Dramatic decrease in hepatic VLDL-TG secretion in *Pdia1*-LKO mice (n = 3). $^{**}P < 0.01$.

Unlike MTTP, PDIA1, also known as prolyl 4-hydroxylase subunit β (P4HB), is ubiquitously expressed and is a member of the thioredoxin superfamily [45–48]. PDIA1 contains four thioredoxin-like domains arranged in the order a, b, b', and a' and an acidic C-terminal region where a KDEL ER retention signal resides [46,47]. Its two catalytic domains (a, a') contain an active site consisting of Cys-Gly-His-Cys residues and are separated by two non-catalytic domains (b, b') [45,46,48,49] (Figure 1A). PDIA1 and ER luminal oxidase 1 ERO1 act in a cycle to promote proper disulfide bond formation during oxidative protein folding [50–52]. Besides its oxidoreductase function, the b and b' domains of PDIA1 can participate as a chaperone to support protein folding independent of its catalytic activity [46,53–55]. *In vitro* studies showed that the isomerase activity of PDIA1 is not required for its interaction with MTTP [56,57]. MTTP does not contain an ER retention motif and presumably, it relies on interaction with PDIA1 for ER residency as well as to maintain its proper conformation. Furthermore, it remains unknown whether other PDI family member thiol isomerases can replace PDIA1 to maintain MTTP function. APOB is a large highly hydrophobic protein, and its folding during VLDL biogenesis requires extensive co- and post-translational modifications of the nascent APOB polypeptide with the participation of many ER molecular chaperones [6,27,58]. Previously, we used rat hepatoma cells to demonstrate that PDIA1 plays an important role in the oxidative folding of APOB100 [59]. In addition, a key conserved UPR sensor IRE1α exerts a regulatory role in hepatic VLDL secretion through inducing PDIA1 expression to impact MTTP activity [23]. However, neither the physiological requirement nor the exact role(s) of PDIA1 in VLDL assembly and secretion are not fully understood.

Global knockout (KO) of *Pdia1* is embryonic lethal [51,60] and as a result, the physiological requirement for PDIA1 function in adult tissues is poorly understood. In this study we generated hepatocyte-specific *P4hb* KO (*Pdai1*-LKO) mice and demonstrate an essential role for PDIA1 in hepatic lipid transport and whole-body lipid homeostasis. These findings establish an indispensable role for PDIA1 in MTTP protein synthesis and function and reveal a novel chaperone function for PDIA1 in VLDL secretion mediated through interaction with the peptide segment between APOB27 and APOB48 in an MTTP-independent manner. Our study provides novel insight into physiological functions for PDIA1 as well as the mechanisms governing VLDL assembly and secretion.

2. MATERIALS AND METHODS

2.1. Reagents

Antibodies used were as follows: rabbit anti-PDIA1 (11245-1-AP), rabbit anti-PDIA3 (15967-1-AP), rabbit anti-PDIA4 (14712-1-AP), and rabbit anti-PDIA6 (18233-1-AP) were from Proteintech (Rosemont, IL). Rabbit anti-BiP (3177), rabbit anti-IRE1α (3294), rabbit anti-phospho IRE1α (9721) and rabbit anti-IRE1α (9722) were from Cell Signaling Technology, (Danvers, MA). Mouse anti-beta actin (PIMA 1140; ThermoFisher, Waltham, MA); mouse anti-MTTP (612022; BD biosciences, San Diego, CA). Goat anti-human apoB (AB742), mouse anti-FLAG (F11804), mouse anti-FLAG magnetic beads (M8823), rabbit anti-albumin (A3293), 2,2′-dipyridyldisulfide (2127-03-9), Peg-Maleimide (712469) were from Sigma (St Louis, MO). Rabbit anti-mouse APOB, rabbit anti-mouse APOE, rabbit anti-mouse APOA1 and rabbit anti-human APOB were described [11,12,17]. C-terminally FLAG-tagged human PDIA1 was a gift from P. Arvan (University of Michigan, Ann Arbor) [61] and human APOB100 cDNA was a gift from Z. Yao (University of Ottawa, Ottawa, Canada) [62]. Expression vector encoding human APOB48 was from Addgene (138334; Watertown, MA). Glycerol [2–3H] (ART 0188A) and EasyTag™ EXPRESS-35S Protein Labeling Mix (NEG77200) were from American Radiolabeled Chemicals (St Louis, MO) and PerkinElmer (Waltham, MA), respectively.

2.2. Mice

C57BL/6 mice with *Pdia1* floxed alleles were obtained from Dr. J Cho (Univ. of Illinois-Chicago) [60]. To induce hepatocyte-specific *Pdia1* deletion, mice were transduced with Ad-Cre [63] ($0.9x\ 10^{10}$ pfu/mouse) or AAV8-TBG-Cre (Addgene, Watertown, MA) ($1x\ 10^{11}$ VG/mouse) at the age of 6–10 wks. Littermates transduced with Ad-βGal [63] ($0.9x10^{10}$ pfu/mouse) or AAV8-TBG-βGal (Addgene) ($1x\ 10^{11}$ VG/mouse) were used as controls. Experiments were performed 6–11 wks post-transduction. All mice were fed with regular mouse chow-diet. Both male and female mice were used in the study. All procedures were performed by protocols and guidelines reviewed and approved by the Institutional Animal Care and Use Committee (IACUC) at the SBP Medical Discovery Institute (AUF # 20–056).

2.3. Construction of recombinant adenoviruses

Ad-GFP, Ad-MTTP, Ad-PDI, and Ad-PDImt were described [23,64]. Ad-hApoB15 and Ad-hApoB27 were prepared using AdTrack-CMV/AdEasy-1 system [17,64]. The cDNA inserts encoding hApoB15 and hApoB27 were prepared from human apoB100-expression vector [62].

2.4. Metabolic labeling studies using primary hepatocytes

Hepatocytes were isolated from the *Pdia1*-LKO or *Pdia1*f/f mice by collagenase perfusion through the portal vein as described [11,23]. They were cultured in collagen-coated 12-well or 6-well culture plates in high glucose DMEM containing 10 % FBS. In experiments involving adenovirus (Ad)-mediated gene delivery, hepatocytes were the transduced with the indicated Ad constructs 16–20 h post attachment at an MOI of 7.

^{35}S-methionine/cysteine-pulse labeling experiments to determine MTTP synthesis were performed on *Pdia1*f/f and *Pdia1*-LKO hepatocytes within 20 h after attachment. The ^{35}S-labeled albumin and MTTP in the cell lysates were immunoprecipitated using rabbit polyclonal anti-human albumin (Sigma), and guinea pig polyclonal anti-mouse MTTP produced by immunizing guinea pig with a recombinant mouse MTTP protein, separated on polyacrylamide gradient SDS-gels (5–12 %) and transferred onto nitrocellulose membranes before being exposed to X-ray films. The intensities of the ^{35}S-labeled MTTP and albumin bands on the X-ray films were quantified using Image J.

^{35}S-methionine/cysteine was used for pulse-chase (pulsed for 30 min, followed by the specified chase time periods) analyses of synthesis and secretion of apoB100 and apoB48 as described [23,64] at 20 h post-attachment for the untransduced primary hepatocytes and at 18 h post-transduction for hepatocytes transduced with Ad-PDI, Ad-PDImt, Ad-MTTP, or Ad-GFP. The chase media contained 0.3 mM BSA-bound oleic acid [11] in these experiments. ApoB and albumin in the cell lysates and chase media were immunoprecipitated using rabbit polyclonal anti-mouse APOB [11,64] and rabbit polyclonal anti-human albumin (Sigma) and the ^{35}S-labeled APOB and albumin were quantified as described above for ^{35}S-labeled MTTP.

To measure rates of synthesis and secretion of TG, at 18 h after transduction with the indicated Ad vectors, hepatocytes were incubated with 2-[^{3}H]-glycerol-containing DMEM (10 μCi/ml) for 4 h with 0.3 mM oleate complexed to BSA [11]. [^{3}H]-labeled TG was isolated from cells and medium and [^{3}H]-radioactivity measured as described [11,23]. Data were expressed as DPM/mg protein/h.

2.5. Determination of liver redox state *ex vivo*

Thin liver slices (~1.5 mM in thick) were prepared from livers of *Pdia1*-LKO or *Pdia1*f/f mice in ice-cold serum-free DMEM. They were transferred into 12-well culture plates (~30 mg/well) containing 2 ml DMEM and incubated in cell culture incubator at 37C for 30 min. The incubation medium was then replaced with prewarmed DMEM containing 0.5 mM DPS, or vehicle and the livers slices were incubated for 5 min. The livers slices were then transferred into new plates containing fresh DMEM and rinsed twice with DMEM and incubated in 2 ml prewarmed DMEM for the indicated time periods. At the end of each of these wash-out incubation time points, the liver slices were immediately lysed in RIPA buffer containing 10 mM Peg-maleimide and 2 x protease inhibitor cocktail (Fisher). The resultant lysates were incubated at room temperature for 30 min. Aliquots of the Peg-maleimide-treated lysates were subjected to SDS-PAGE under reducing conditions and immuno-blotted with the specified primary antibodies.

2.6. Liver immunohistochemistry

Livers were harvested and fixed in 4 % PFA. Paraffin embedding, sectioning, and slide preparations were performed in the SBP Histopathology Core Facility. Sections were stained with the following antibodies: guinea pig polyclonal anti-mouse MTTP, rabbit polyclonal anti-PDIA1 (Proteintech, 11245−1-AP), rabbit polyclonal anti-4-HNE [65], anti-F4/80, and DAPI (Fisher Scientific). For secondary antibodies, Alexa Fluor 488 goat a-rabbit IgG, and Alexa Fluor 594 goat a-guinea pig IgG anti-bodies were used (Invitrogen). Images were taken by a Zeiss LSM 710 confocal microscope with a 40X objective lens.

2.7. Transmission electron microscopy

Samples were prepared according to the UCSD Cellular and Molecular Medicine Electron Microscopy Facility protocols. Livers were perfused in modified Karnovsky's fixative (2.5 % glutaraldehyde and 2 % paraformaldehyde (PFA) in 0.15M sodium cacodylate buffer, pH 7.4) and fixed for at least 4 h, post-fixed in 1 % osmium tetroxide in 0.15M cacodylate buffer for 1 h and stained *en bloc* in 2 % uranyl acetate for 1 h. Samples were dehydrated in ethanol, embedded in Durcupan epoxy resin (Sigma−Aldrich, Inc St. Louis), sectioned at 50−60 nm on a Leica UCT ultramicrotome, and delivered to Formvar and carbon-coated copper grids. Sections were stained with 2 % uranyl acetate for 5 min and Sato's lead stain (Sato, 1968) for 1 min. Images were obtained using a Tecnai G2 Spirit BioTWIN transmission electron microscope equipped with an Eagle 4 k HS digital camera (FEI, Hillsboro, OR) with indicated magnifications.

2.8. Western blotting

Liver and primary hepatocytes lysates were prepared in RIPA buffer (10 mM Tris pH 7.4, 150 mM NaCl, 0.1 % SDS, 1 % NP-40, 2 mM EDTA) with protease and phosphatase inhibitors (Fisher Scientific) on ice for 10 min and lysates were collected after centrifugation at 4 °C for 5 min at 10000×*g*. Sample proteins were separated on polyacrylamide gradient SDS-gels (4−12 %) under reducing conditions and transferred to nitrocellulose membranes (Bio-Rad Laboratories, Inc). After blocking and incubation with the specified primary antibodies, specific bands were detected and quantified using fluorescent-labeled secondary antibodies and LiCor system (LI-COR Biosciences, Lincoln, NE).

2.9. Analysis of APOB-PDIA1 interaction using cDNA-transfected COS-7 cells

Adenoviruses expressing human APOB15 (amino acids 1−693 of APOB100) or APOB27 (amino acid 1−1254 of APOB100) were generated by PCR-cloning of the respective coding region of human APB100 cDNA [62] and subcloned into AdTrack-CMV-GFP at the *Kpn*1 and *Not*1 restriction sites, followed by production of recombinant adenoviral vectors using AdEasdy-1 system [17,64]. Catalytically inactive FLAG-tagged PDIA1 expression vector was prepared by converting all 4 Cys residues (Cys53, Cys 56, Cys 397 and Cys 400) in the catalytic sites of FLAG-tagged human PDIA1 [61] to Ser residues using a Q5® Site-Directed Mutagenesis Kit (NEB, Ipswich, MA). cDNA vector transfection into COS-7 cells was performed using Turbofect transfection reagent (ThermoFisher). Cells were harvested at 40 h after cDNA vector transfection and adenoviral transduction. Cell lysates were prepared in a lysis buffer containing 0.15 mM NaCl, 0.5 % Triton X-100, 20 mM HEPES, pH 7.4, 1x Protease inhibitor cocktail (ThermoFisher). FLAG-IP was performed using anti-FLAG M2 magnetic beads (Sigma).

2.10. RNA isolation and RT-qPCR

Total RNAs were extracted from liver samples using RiboZol Extraction reagent (VWR Life Science). Reverse transcription reactions were performed using iScript cDNA Synthesis kit (Bio-Rad Laboratories, Inc). The relative mRNA levels were measured by qPCR with iTaq Universal SYBR green Supermix (Bio-Rad Laboratories, Inc).

2.11. Miscellaneous procedures

MTTP activity in hepatocyte lysates was measured with a fluorescent assay kit (Sigma) according to the manufacturer's protocol and as described [23,64].

Plasma samples were obtained from mice after a 4-h fasting. Plasma TG and cholesterol levels were measured using Infinity kits (Fisher).

Rates of hepatic TG secretion were determined as described [23,64] except that poloxamer 407 [66] instead Triton WR-1339 was used to block VLDL clearance *in vivo*.

Liver TG content was directly measured in liver homogenates as described [23,64].

2.12. Statistical analysis

Data are indicated as Mean ± SEM. Statistical significance was evaluated by unpaired two-tailed Student's t test. P-values are presented as $*p < 0.05$, $**p < 0.01$.

3. RESULTS

3.1. Hepatocyte-specific Pdia1 deletion induces severe hypolipidemia and hepatic steatosis coupled with defective VLDL-TG secretion

The embryonic lethality of germline *Pdia1* deletion in mice led us to generate *Pdia1-LKO* mice to investigate its role in hepatic lipid metabolism. For this purpose, we transduced mice homozygous for floxed *Pdia1*-alleles (*Pdia1*$^{f/f}$) [60] with either Ad-CMV-Cre or AAV serotype 8 (AAV8) vectors that bear a thyroxine binding globulin (TBG) promoter-driven Cre recombinase (AAV8-TBG-Cre) to induce hepatocyte-specific deletion of *Pdia1*, with Ad-CMV-βGal- or AAV8-TBG-βGal-transduced *Pdia1*$^{f/f}$ littermates as controls (Figure 1A). Ad-Cre-mediated *Pdia1*-deletion reduced liver *Pdia1* mRNA and protein by 75−80 % (Figure 1 supplement 1A) whereas transduction of *Pdia1*$^{f/f}$ mice with AAV8-TBG-Cre-almost eliminated both *Pdia1* mRNA and its protein product in the liver (Figure 1B−C). Hepatocyte-specific *Pdia1* deletion did not affect mRNA levels of *Pdia3*, *Pdia4* or *Pdia6* (Figure 1B) but modestly increased the level of hepatic PDIA4 protein (Figure 1C). AAV8-TBG-Cre was used to induce hepatocyte-specific *Pdia1* deletion in the *Pdia1*$^{f/f}$ mice throughout this study unless otherwise specified in experiments where Ad-Cre was used.

Pdia1 deletion in hepatocytes did not affect body weight, blood glucose, with a slight increase in plasma ALT level (Figure supplement 1B-D). However, both plasma TG and cholesterol levels were dramatically reduced in the *Pdia1*-LKO mice (Figure 1D), accompanied by almost complete absence of plasma ApoB100, ApoB48 and ApoE (Figure 1E,F). Plasma ApoA1 was also greatly reduced (Figure 1E,F). Plasma albumin levels were not altered upon *Pdia1* deletion (Figure 1E), suggesting no gross impairment of the functional secretory pathway. The plasma samples for these analyses were obtained after fasting the mice for 4 h to deplete circulating intestinal lipoproteins. The absence of plasma ApoB100 and ApoB48 in the *Pdia1*-LKO mice indicates a block in their secretion the PDIA1-ablated hepatocytes. On the other hand, while secretion of ApoA1 and ApoE does not rely on the VLDL assembly and secretion processes, disruption in hepatic VLDL secretion is known to greatly reduce plasma HDL and ApoA1 levels in *Mttp*- or *Apob*-targeted mice [11,12,40] because plasma VLDL is a major lipid source for HDL maturation in the plasma without which ApoA1 is rapidly catabolized. Inhibition of hepatic VLDL secretion also accelerates clearance of ApoE from the plasma in mice [11,12,67].

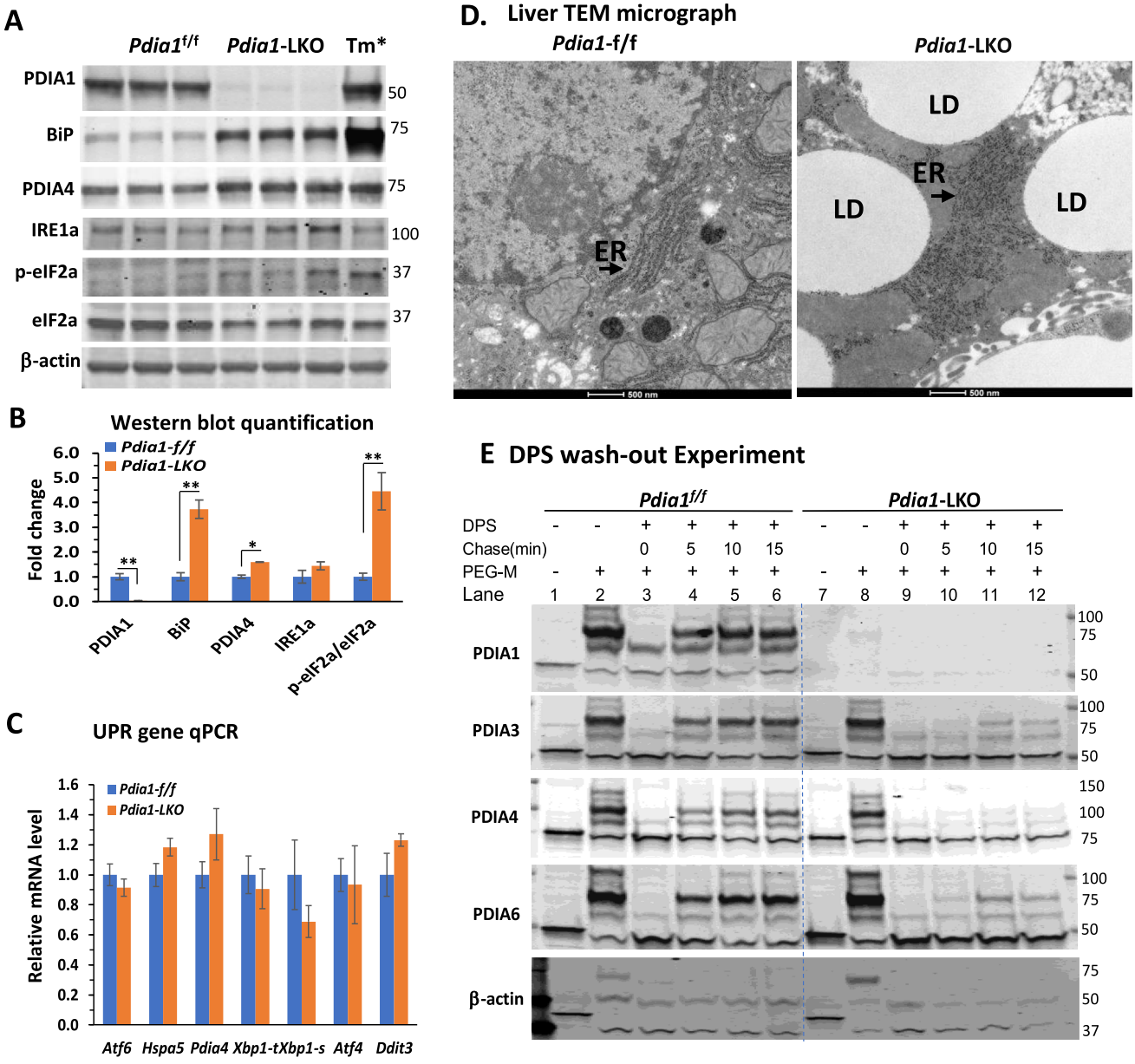

Figure 2: Hepatocyte-specific deletion of *Pdia1* causes ER stress and alters the redox state in the ER without discernible change in ER morphology. **A**, **B**. Increased cellular levels of BiP, PDIA4, and p-eIF2α in livers of *Pdia1*-LKO mice. Each lane represents an individual mouse (label lane numbers). TM*, liver lysate from a tunicamycin (TM)-treated mouse was used as a positive control for UPR activation. **C.** *Pdia1*-deletion did not alter mRNA levels for key UPR sensors (n = 5). **D**. TEM analysis revealed no detectable difference in the ER morphology comparing livers of *Pdia1*$^{f/f}$ and *Pdia1*-LKO mice. Scale bar: 500 nm. LD, lipid droplet. **E.** Assessment of the redox state in the ER in liver slices of *Pdia1*$^{f/f}$ and *Pdia1*-LKO mice using a 2,2′-dipyridyldisulfide (DPS)-treatment and washout procedure in combination with tagging the free thiol groups with Peg-maleimide (PEG-M). The return of PDIA3 and PDIA4 to their reduced forms after oxidative treatment with DPS was slightly delayed in *Pdia1*-LKO liver slices (Lane 10) compared to the *Pdia1*$^{f/f}$ liver slices (lane 4), indicating an increased oxidative state in the ER of *Pdia1*-LKO livers. *, P $<$ 0.05; **, P $<$ 0.01.

Importantly, hepatocyte-specific *Pdia1* deletion induced severe hepatic steatosis (Figure 1G), with an 8-10-fold increase in hepatic TG content (Figure 1H), that correlated with an 85 % decrease in hepatic VLDL-TG secretion in *Pdia1*-LKO mice (Figure 1I). Together, these results demonstrate an essential role for PDIA1 in hepatic VLDL secretion and lipid homeostasis. In addition, the findings in these chow-fed *Pdia1*-LKO mice generally phenocopy mice with liver specific *Mttp* deletion [40,68,69].

3.2. Pdia1-deletion modestly activates UPR signaling and alters ER redox status in hepatocytes without eliciting major ER ultrastructural alterations

Given its high expression level in hepatocytes and its critical role in oxidative protein folding in cultured cells [45,47,70], we tested the impact of *Pdia1*-deletion on hepatocyte function *in vivo* using the *Pdia1*-LKO mice. In response to *Pdia1*-deletion, BiP content in the *Pdia1*-LKO livers was increased 3.7-fold, with a 1.5-fold increase in PDIA4 level (Figure 2A–B). There were no discernible changes in IRE1α. However, eIF2α phosphorylation, a transducer of the integrated stress response, was significantly induced in the *Pdia1*-LKO livers (Figure 2A–B). In contrast to these changes in UPR signaling at the protein level, there were no alterations in the mRNA levels of all key UPR sensors tested, including *Hspa5*, *Pdia4* and *Xbp1-s* (Figure 2C). We also assessed the potential impact of *Pdia1*-deletion on hepatocyte ultrastructure by transmission electron microscopy (TEM). However, TEM analysis of *Pdia1* LKO hepatocytes revealed cytosolic lipid-droplet accumulation but did not cause discernible ER distension or vesiculation (Figure 2D). Furthermore, pulse-chase analysis did not reveal any detectable changes in total protein synthesis or secretion by PDIA1-ablalated hepatocytes (Figure supplement 2A).

To determine whether elimination of PDIA1 affects ER redox status, we performed 2,2′-dipyridyldisulfide (DPS)-washout experiments on liver slices of *Pdia1*$^{f/f}$ and *Pdia1*-LKO mice. Incubation of liver slices with DPS causes oxidation of thiol groups that can be reversed after removal of DPS, depending on the redox status of the cell [49]. Peg-maleimide was used to tag the free thiol groups at different time points after DPS oxidation, *i.e.,* restoring the reduced state. In the absence of DPS pretreatment, Peg-maleimide (MW 10—15 kDa) reactivity reduced migration of PDIA1, PDIA3, PDIA4 and PDIA6 on SDS-PAGE under reducing conditions (Figure 2E, lanes 2 and 8). Pretreating the liver slices with DPS (without DPS washout) almost completely blocked labeling of the PDI proteins with Peg-maleimide (Figure 2E, lanes 3 and 9). A 5-min

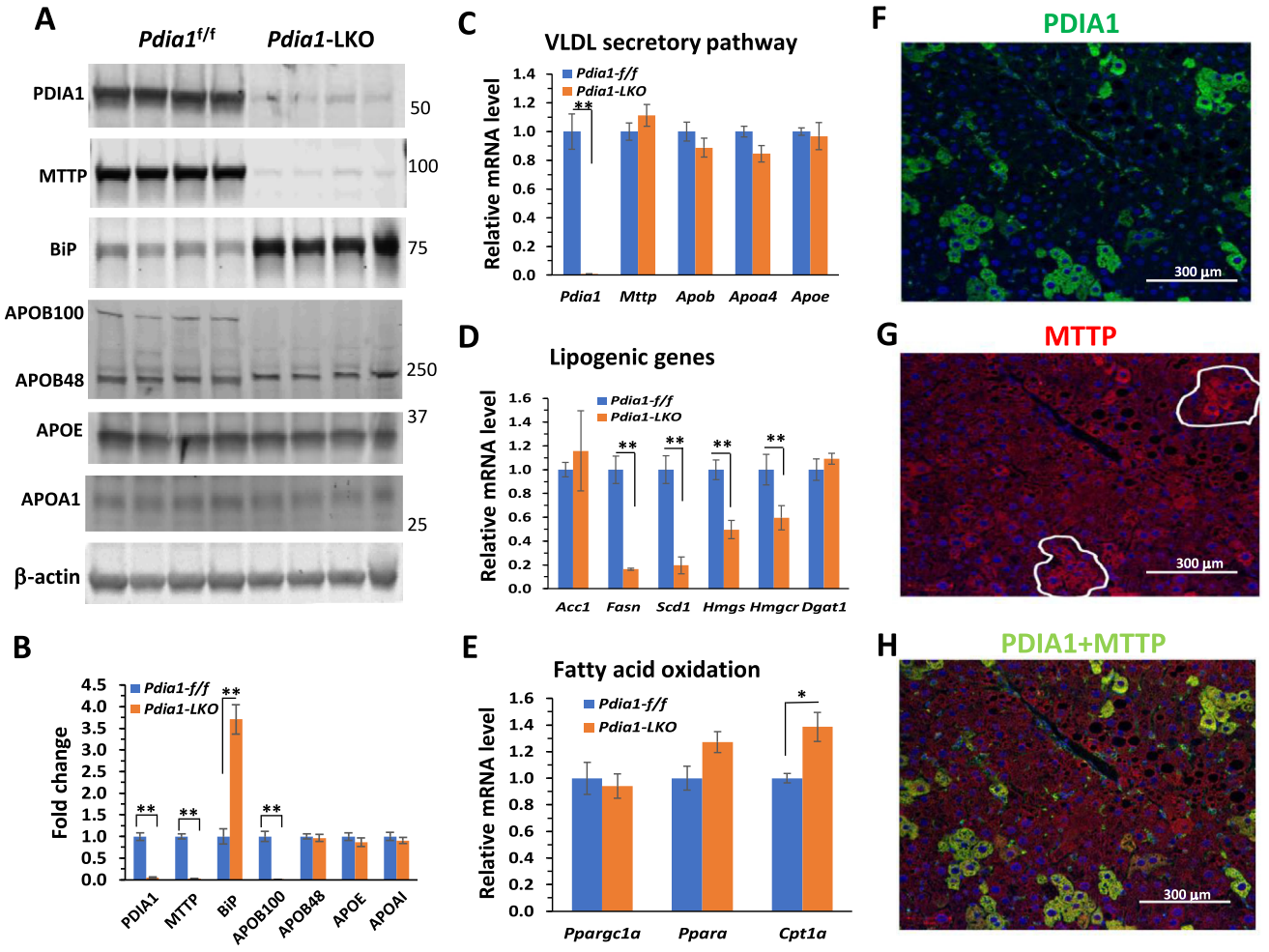

Figure 3: PDIA1 ablation leads to disappearance of MTTP without affecting its mRNA level in the liver. A, **B**. Western blot analysis revealed near absence of both MTTP and APOB100 in the livers of *Pdia1*-LKO mice. Each lane represents an individual mouse. **C.** mRNA levels of *Mttp* and the VLDL-apolipoprotein genes were not altered in response to *Pdia1*-deletion (n = 5). *Pdia1*-deletion reduced expression of lipogenic genes (**D**) and upregulated the fatty acid oxidation pathway (**E**). Immunofluorescence analysis (**F, G, H**) of a partially *Pdia1*-deleted liver demonstrated co-localization of MTTP and PDIA1 in the PDIA1-positive hepatocytes, but loss of MTTP in the *Pdia1*-deleted hepatocytes.

washout almost completely restored the Peg-maleimide labeling of the PDI's in the DPS-treated *Pdia1*$^{f/f}$ liver slices (Figure 2E, lanes 4), compared to greater than 10 min for the DPS-treated *Pdia1*-LKO liver slices (Figure 2E, lanes 11). These findings indicate that *Pdia1*-deletion may render the ER more oxidative, which may in turn increase the susceptibility of *Pdia1*-deleted hepatocytes to oxidative stress. However, staining of the liver sections of the *Pdia1*-LKO mice (6 weeks post induction of *Pdia1*-deletion) with a 4-hydroxynonenal antibody for lipid peroxides did not show any sign of increased oxidative damage to lipids (Figure supplement 2B). In addition, based on F4/80 staining, *Pdia1*-deletion did not elicit discernible inflammation in the *Pdia1*-LKO livers (Figure supplement 2C). Thus, except for inducing severe hepatic steatosis, *Pdia1* deletion in hepatocytes did not cause any other detectable pathological changes in the livers of the *Pdia1*-LKO mice fed a regular mouse chow-diet.

3.3. Hepatocyte Pdia1 deletion eliminates MTTP protein without affecting mRNA expression

To delineate the mechanism underlying defective VLDL secretion upon hepatocyte specific *Pdia1* deletion, we first analyzed mRNA and protein expression for selective components of the VLDL biogenesis machinery. *Pdia1*-deletion reduced hepatic abundance of ApoB100, but not ApoB48, ApoE or ApoA1 proteins (Figure 3A—B). In addition, and to our surprise, MTTP was virtually absent in livers of *Pdia1*-LKO mice (Figure 3A—B). *Pdia1*-deletion did not alter mRNA levels of any of the VLDL apolipoprotein genes (Figure 3C). Consistent with our previous report that disruption of VLDL secretion in *Apob*-targeted mice suppressed lipogenesis but induced mitochondrial fatty acid β-oxidation in the liver [71], *Pdia1*-deletion reduced expression of most of the lipogenic genes tested (Figure 3D), with a modest induction of genes encoding fatty acid oxidation including *Ppara* and *Cpt1a* (Figure 3E). Despite that MTTP is absent in *Pdia1*-deleted hepatocytes, *Pdia1*-deletion did not alter *Mttp* mRNA expression (Figure 3C), suggesting that *Pdia1*-elimination depleted MTTP protein at a post-transcriptional level. Immunofluorescence co-localization of PDIA1 and MTTP in liver sections with incomplete *Pdia1*-deletion induced via Ad-CMV-Cre transduction, demonstrated MTTP was present in the PDIA1-positive hepatocytes and not in the *Pdia1*-deleted hepatocytes (Figure 3F—H), confirming our conclusion based on the results from immunoblot analysis (Figure 3A—B) that MTTP is absent in *Pdia1*-deleted hepatocytes.

3.4. Inhibition of MTTP mRNA translation and not MTTP degradation causes MTTP depletion in Pdia1-deleted hepatocytes

To test whether *Pdia1*-deletion destabilizes MTTP protein in hepatocytes, we transduced *Pdia1*$^{f/f}$ and *Pdia1*-deleted primary hepatocytes with Ad-GFP or Ad-MTTP and subsequently treated the hepatocytes with MG132 or MG132 plus chloroquine for 8 h to inhibit MTTP proteasomal and lysosomal degradation. However, neither treatment rescued MTTP expression in *Pdia1*-deleted hepatocytes that were transduced with Ad-GFP or Ad-MTTP (Figure 4A). We then treated Ad-GFP- or Ad-MTTP-infected *Pdia1*-deleted primary hepatocytes with cycloheximide (CHX) to inhibit translation to directly measure the rate of MTTP decay. CHX treatment for up to 14 h did not significantly alter MTTP protein levels

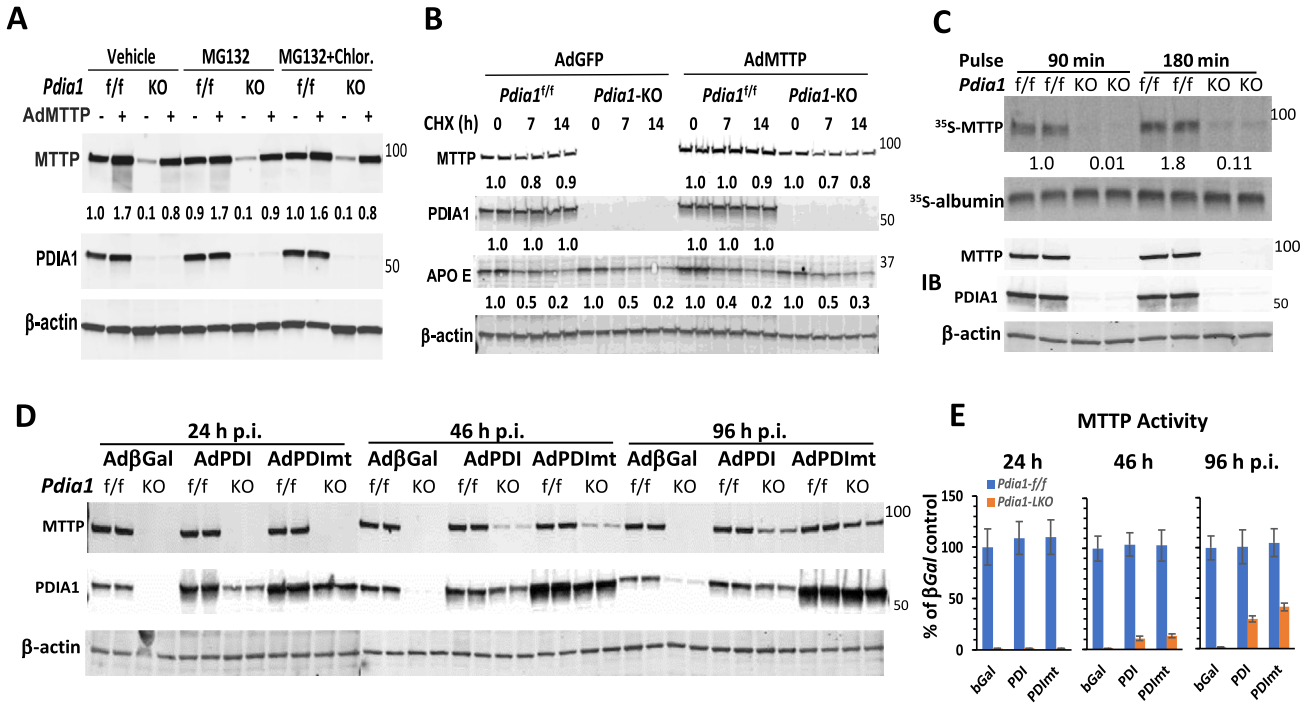

Figure 4: Inhibition of MTTP mRNA translation causes MTTP depletion in *Pdia1*-deleted hepatocytes. A. MTTP was forcibly expressed in *Pdia1*-deleted hepatocytes by Ad-MTTP transduction and MTTP stability was analyzed in the presence or absence of MG132 (20 μM) with or without chloroquine (100 μM) for 8 h. Inhibition of proteasome or lysosomal degradation did not stabilize endogenous or exogenous MTTP. **B**. MTTP decay was analyzed by cycloheximide (CHX, 100 μM) to inhibit MTTP synthesis in Ad-GFP- or Ad-MTTP-transduced *Pdia1*$^{f/f}$ and *Pdia1*-deleted (*Pdia1*-KO) hepatocytes. No difference was observed in the rate of MTTP decay between the two genotypes. Decay of intracellular ApoE was used as positive control for cycloheximide-treatment. **C.** Metabolic labeling with ^{35}S-Met/Cys revealed that synthesis of MTTP was significantly inhibited in *Pdia1*-deleted (KO) hepatocytes. Each lane represents hepatocytes isolated from separate mice. **D**. Complementary expression of wild type PDIA1 (Ad-PDI) or catalytically inactive PDIA1 (Ad-PDImt) in *Pdia1*-deleted hepatocytes did not rescue MTTP protein or MTTP activity (**E**) during the first 24 h post infection (p.i.). However, both MTTP protein and activity was detected at 46 h p.i. and much higher levels at 96 h p.i. of Ad-PDI or Ad-PDImt (**E**).

(Figure 4B) whereas the decay of intracellular ApoE was evident in both *Pdia1*$^{f/f}$ and *Pdia1*-deleted hepatocytes. These results are consistent with the notion that MTTP has a very slow turnover rate ($t_{1/2}$ = 4–5 days) in hepatocytes [72,73] as well as for the MTTP produced through forced expression in the absence of PDIA1. Thus, the absence of MTTP in the *Pdia1*-deleted hepatocytes is unlikely due to its enhanced degradation due to depletion of the PDIA1 subunit.

Metabolic labeling of *Pdia1*$^{f/f}$ and *Pdia1*-deleted primary hepatocytes with [^{35}S]-Met/Cys revealed that MTTP synthesis in *Pdia1*-deleted hepatocytes was reduced to ~5 % of that of the *Pdia1*$^{f/f}$ hepatocytes (Figure 4C). Together, these results support the notion that inhibition of MTTP synthesis is the key mechanism whereby *Pdia1*-deletion depletes MTTP.

To test whether complementary expression of intact PDIA1 or an enzymatically inactive PDIA1 mutant (PDImt) in which all 4 cysteine residues in the catalytic sites were converted to serine residues [23] can rescue MTTP expression in the *Pdia1*-deleted hepatocytes, we transduced the *Pdia1*$^{f/f}$ and *Pdia1*-deleted primary hepatocytes with adenoviruses expressing PDI (Ad-PDI) or PDImt (Ad-PDImt) and determined their effects on MTTP levels. We observed that complementary expression of PDI or PDImt did not rescue MTTP protein or activity in *Pdia1*-deleted hepatocytes at least 24 h post-transduction (Figure 4D–E). However, by 96 h post-transduction, expression of either PDI or PDImt partially rescued MTTP protein synthesis and activity in *Pdia1*-deleted hepatocytes (Figure 4D–E), demonstrating that the isomerase function of PDIA1 is not required for MTTP synthesis and function.

3.5. The chaperone activity of PDIA1 is required for APOB48 secretion independent of its role in MTTP function

Previous studies demonstrated that elimination of MTTP function preferentially blocks secretion of murine APOB100 [40,68]. The near complete absence of both circulating ApoB100 and ApoB48 in the *Pdia1*-LKO mice (Figure 1E) indicates that secretion of both ApoB100 and ApoB48 is blocked in hepatocytes in the absence of hepatocyte PDIA1. Indeed, pulse-chase analysis of *Pdia1*-deleted hepatocytes

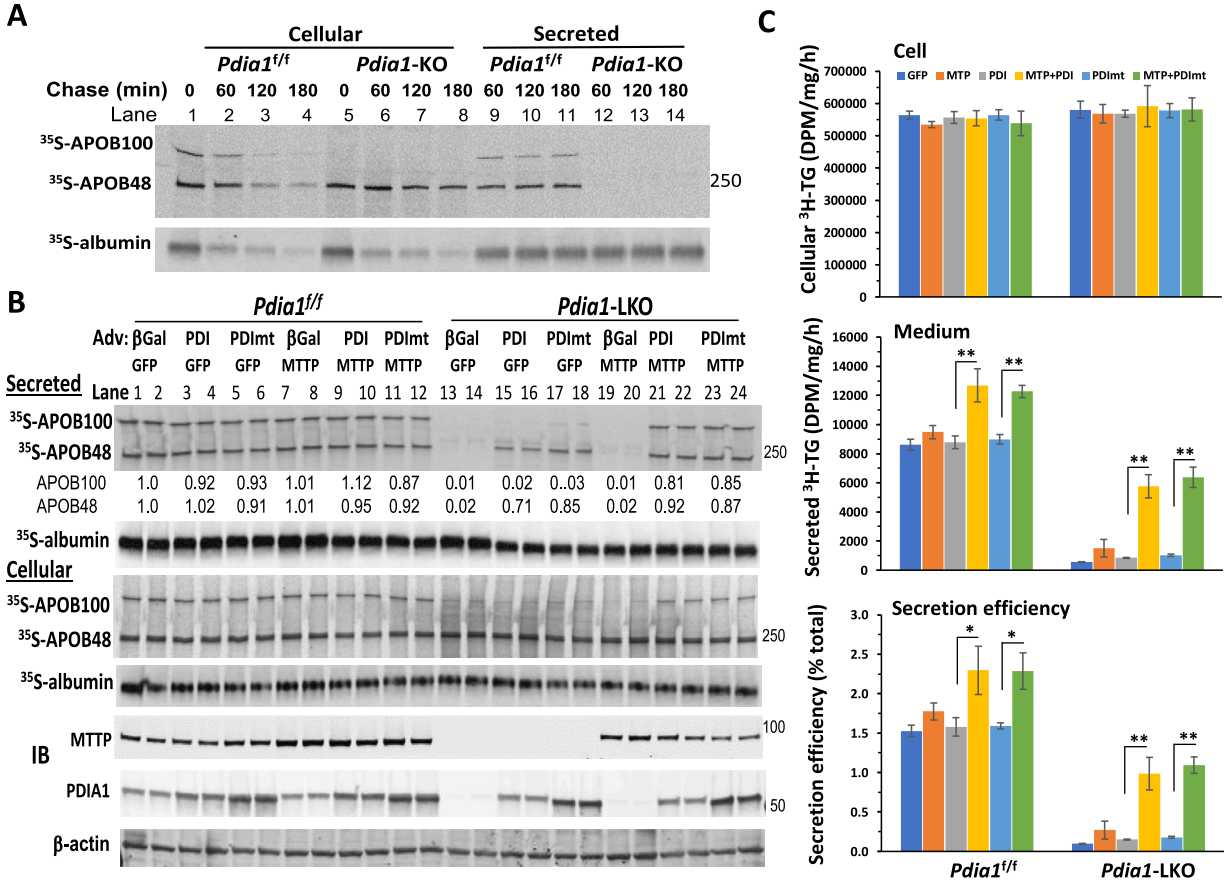

Figure 5: Secretion of APOB48 is completely blocked in *Pdia1*-deleted hepatocytes and is rescued by complementary expression of wild type PDIA1 (PDI) or catalytically inactive PDIA1 (PDImt). A. Pulse-chase analysis revealed that *Pdia1*-deletion did not affect APOB48 synthesis (lane 5 vs lane 1) but it completely inhibited APOB48 secretion (lanes 12–14 vs lanes 9–11, respectively). **B**. Complementary expression of PDI or PDImt alone rescued APOB48 secretion. Hepatocytes isolated from *Pdia1*$^{f/f}$ and *Pdia1*-LKO mice were infected with the indicated adenoviruses at 20 h after plating. At 18 h post-transduction, the hepatocytes were pulse-labeled with ^{35}S-Met/Cys in the presence of 0.3 mM oleic acid complexed with BSA (OA-BSA) for 3 h. The ^{35}S-labeled ApoB's and albumin were immunoprecipitated with rabbit polyclonal antibodies against mouse APOB and albumin, respectively. Immunoblotting (IB) demonstrated that no endogenous MTTP was rescued in the Ad-PDI- or Ad-PDImt-infected *Pdia1*-LKO hepatocytes. **C.** Complementary expression of PDI or PDImt alone did not rescue secretion of ^{3}H-labeled TG by the *Pdia1*-LKO hepatocytes, neither did forced expression of MTTP alone. Hepatocytes isolated from *Pdia1*$^{f/f}$ and *Pdia1*-LKO mice were infected with the indicated adenoviruses. At 18 h p.i., hepatocytes were incubated with DMEM containing 0.3 mM oleic acid-BSA and ^{3}H-glycerol for 4 h. The ^{3}H-labeled TG in cells and media were isolated and the ^{3}H-radioacivity was measured and expressed as DPM/mg cell protein/h. Each bar represents average +/− SD of triplicate wells. *, $P < 0.05$; **, $P < 0.01$.

demonstrated that while ApoB48 synthesis is not altered (Figure 5A, lane 1 vs lane 5), ApoB48 secretion is completed prevented (Figure 5A, lanes 12—14). Complementary expression of PDI or PDImt, but not MTTP, rescued ApoB48 secretion as early as 18h post-transduction (Figure 5B, top panel lanes 13—20) despite the finding that MTTP expression was not rescued in the AdPDI- or AdPDImt-transduced *Pdia1*-deleted hepatocytes at this time point (Figure 5B, lanes 13—18 in IB panels). This finding suggests a new and unanticipated role for PDIA1 in supporting the folding and secretion of APOB48, which functions in both an MTTP-independent and PDIA1-isomerase activity-independent manner. However, while expression of either PDI or PDImt rescued APOB48 secretion in the *Pdia1*-deleted hepatocytes at the 18 h time point, TG secretion was not rescued in the absence of MTTP (Figure 5C). As expected, co-transduction of *Pdia1*-deleted hepatocytes with AdMTTP and AdPDI or AdPDImt restored secretion of both APOB isoforms along with TG (Figure 5B—C). These findings support the concept that murine hepatic APOB48 and TG secretion likely involves distinct pathways within the ER. Indeed, we previously showed that while murine hepatocytes secrete APOB100 solely as VLDL, nearly half of the APOB48 molecules synthesized by murine hepatocytes are secreted as lipid-poor lipoprotein particles with a buoyant density in the high-density lipoprotein range [23,74].

Brodsky and colleagues previously demonstrated that PDIA1 directly interacts with APOB29 through its chaperone activity in a yeast system [75]. The ability of PDImt to support APOB48 secretion in the absence of MTTP suggests that PDIA1 may directly interact with APOB48 to assist folding through its chaperone activity. To test this possibility, we co-transfected COS-7 cells with human APOB48 and FLAG-tagged PDI or PDImt. COS-7 cells do not express MTTP. FLAG-pulldown analyses demonstrated a potential direct interaction of both PDI and PDImt with APOB48 without the participation of MTTP (Figure 6A, lanes 10—13). In contrast to APOB48, neither APOB15 nor APOB27 detectibly interacted with PDI or PDImt in the absence of MTTP (Figure 6B). Furthermore, APOB15 and APOB27 were both readily secreted when expressed from *Pdia1*-deleted hepatocytes using adenoviral vectors (Figure 6C, lanes 11 and 12). Together, these results suggest that ApoB sequences between APOB27 and APOB48 may directly interact with the chaperone domains of PDIA1.

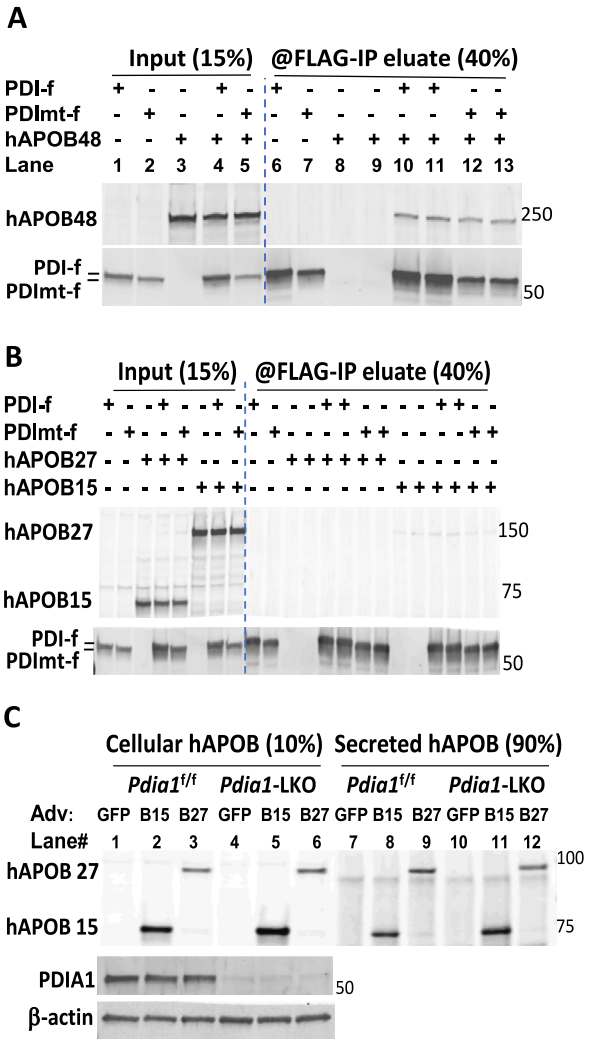

Figure 6: Wild type PDIA1 (PDI) and catalytically inactive PDIA1 (PDImt) directly interact with the peptide region between APOB27 and APOB48, respectively. A. PDI and PDImt interact with APOB48 in transfected COS-7 cells. COS-7 cells were transfected with human APOB48 (hAPOB48), C-terminal-FLAG-tagged PDI (PDI-f) or PDImt (PDImt-f) expression vectors as indicated. The transfected cells were harvested 30 h post-transfection and subjected to FLAG-immnunoprecipitation (IP) analysis using M2 anti-FLAG magnetic beads. Co-IP of hAPOB48 with PDI-f (lanes 10 & 11) or PDImt-f (lanes 12 & 13) indicate their direct interactions. **B.** Neither APOB17 nor APOB27 interact with PDI or PDImt. COS-7 cells were transfected PDI-f or or PDImt-f expression vectors in the presence of Ad-hAPOB15 (hAPOB15) or Ad-hAPOB27. FLAG-IP assays were performed on the DNA transfected COS-7 cells at 30 h post-transfection. No hAPOB15 nor hAPOB27 were pulled down with PDI-f or PDImt-f. **C.** PDIA1 is not required for secretion of APOB17 and APOB27. Hepatocytes isolated from *Pdia1*$^{f/f}$ and *Pdia1*-LKO mice were transduced with Ad-GFP (GFP), Ad-hAPOB15 (B15), or Ad-hAPOB27 (B27). At 48 h post-transduction, hepatocytes, and conditioned media (20 h incubation time) were harvested. Cellular and secreted human ApoB15 and apoB27 were immunoprecipitated with rabbit anti-human ApoB followed by immunoblot analysis using goat anti-human ApoB.

4. DISCUSSION

PDIA1 is a key member of the ER oxidoreductase protein family and is highly expressed in most mammalian tissues. However, little is known about the organ requirement for PDIA1 function *in vivo*. In addition to its protein disulfide isomerase function, one of the distinct biochemical functions of PDIA1 is its role as a subunit of the MTTP complex which plays essential roles in biogenesis and secretion of hepatic VLDL [6,14,40,73]. To establish the physiological functions of PDIA1, we generated *Pdia1*-LKO mice to elucidate its role in hepatic metabolism. Deletion of *Pdia1* in hepatocytes did not have any detectable impact on ER function or general protein synthesis and secretion. Instead, our study reveals that PDIA1 is an indispensable component of the MTTP complex and exerts an obligatory role in hepatic VLDL biogenesis and maintenance of lipid homeostasis in the liver. Importantly, we also identified an essential role for the chaperone function of PDIA1 in mediating ApoB48 folding and its secretion, independent of its role in MTTP function. Thus, in addition to APOB and MTTP, PDIA1 is also an essential genetic requirement for VLDL production (Figure 7). Ablation of PDIA1 in hepatocytes induces PDIA4 expression without affecting expression of PDIA3 and PDIA6 in the murine liver, thus the roles of PDIA1 in MTTP and APOB folding cannot be replaced by these PDI isoforms. Our study highlights new and unsuspected complexity in hepatic VLDL secretion and the regulation of both MTTP expression and function as well as TG independent functions in APOB secretion. *Pdia1* deletion in hepatocytes disrupts hepatic VLDL-TG secretion and induces hepatic steatosis and severe hypolipidemia in the *Pdia1*-LKO

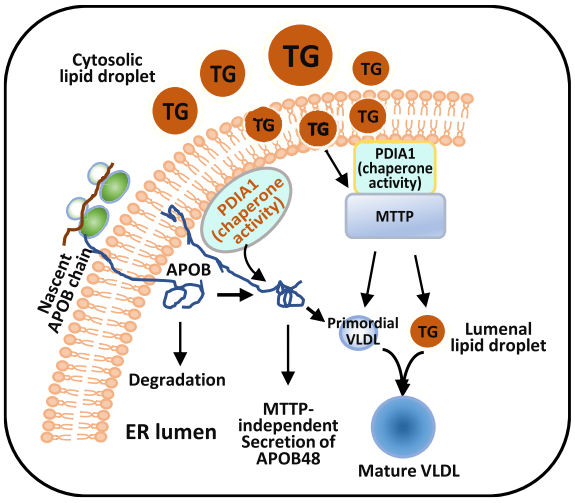

Figure 7: A diagram depicting the obligated roles of chaperone activity of protein disulfide isomerase A1 (PAID1), apolipoprotein B (APOB) and microsomal triglyceride transfer protein (MTTP) in biosynthesis and secretion of hepatic APOB-containing lipoproteins.

mice (Figure 1). Interestingly, we found that along with PDIA1 ablation in murine liver, MTTP is absent in the *Pdia1*-LKO hepatocytes (Figure 3), leading to disruption of hepatic VLDL-TG secretion in these mice. The level of hepatic *Mttp* mRNA was not affected by *Pdia1* deletion (Figure 3C) and there was no detectable MTTP aggregation in the *Pdia1*-LKO hepatocytes (Figure 3). Instead, we provide evidence demonstrating that inhibition of MTTP mRNA translation is the main cause for the absence of MTTP in response to *Pdia1* deletion in murine hepatocytes (Figure 3). We also provide data indicating that PDIA1 ablation does not accelerate MTTP degradation (Figure 4). MTTP has a slow turn-over rate in the liver, with a $t_{1/2}$ of 4–5 days [72,73]. Thus, it took at least 48 h to observe any MTTP in the *Pdia1*-deleted hepatocytes after complementary expression of PDI or PDImt (Figure 4D). Nonetheless, our results do show that both PDI and PDImt are equally effective in rescuing MTTP function in the *Pdia1*-deleted hepatocytes, confirming the notion that the isomerase activity of PDIA1 is not required for the assembly of the MTTP complex [56,57,73]. Our study provides unequivocal evidence for the indispensable role of PDIA1 in MTTP synthesis and function *in vivo*.

While the impact of PDIA1 ablation on MTTP function was predicted based on previous studies [56,57,73], we were surprised to find that the chaperone function of PDIA1 also plays a direct and indispensable role in the folding and secretion of APOB48. Inactivation of MTTP, either by genetic deletion of *Mttp in vivo* or by pharmacological inhibition of MTTP activity in cell culture *in vitro*, can preferentially block APOB100 secretion, [40,43,73]. Here we found that secretion of both APOB100 and APOB48 from the *Pdia1*-deleted hepatocytes were completely disrupted (Figure 5A). We were able to partially rescue secretion of APOB48 but not TG in *Pdia1*-deleted hepatocytes following delivery of either PDI or PDImt at a time point when MTTP expression was not detected (Figure 5). These findings suggest that PDIA1 plays an essential role in APOB48 folding and secretion in the absence of MTTP function. We further demonstrated that PDIA1 interacts with APOB48, but not APOB27 nor APOB15, in a catalytic activity-independent manner without the involvement of MTTP (Figure 6). Unlike APOB48, secretion of APOB27 and APOB15 did not require PDIA1. Consistent with the notion that APOB100 is rapidly degraded in the absence of MTTP, we found that short-term complementary expression of PDI or PDImt alone cannot rescue APOB100 in the *Pdia1*-deleted hepatocytes because ApoB100 is rapidly degraded in the absence of MTTP function. Thus, we were not able to assess the interaction of PDIA1 with APOB100 using transfected COS-7 cells. However, it is possible that the chaperone domain(s) of PDIA1 also interact with APOB100 in an MTTP-independent manner to assist its folding to support ApoB-VLDL secretion. Taken together, our findings demonstrate an essential role for the PDIA1 in APOB folding as well as serving as a subunit of the MTTP complex to support VLDL production. As we previously demonstrated that *Pdia1* expression is regulated by UPR signaling [23,76], it remains to be understood if PDIA1 plays any regulatory role in hepatic lipid metabolism during the pathogenesis of liver disease.

The current study was aimed to understand the role of PDIA1 in hepatic VLDL assembly and secretion and we have yet to use our *Pdia1*-LKO mice to understand the other functions of PDIA1 in the liver. It will be important to investigate what other ER and secretory proteins rely on PDIA1 for their proper folding and secretion by hepatocytes. In conclusion, by using *Pdia1*-LKO mice, we have defined an essential role of PDIA1 in hepatic VLDL secretion and lipid homeostasis. Further studies with this mouse model will likely provide novel insights into the physiological function of PDIA1 in protein folding and secretion.

AUTHOR CONTRIBUTIONS

Z.C., S.W. and R.J.K. conceived the project, Z.C. and R.J.K. designed and interpreted experiments and wrote the manuscript. Z.C., S.W., A.P., A.D. and I.J. performed hepatocyte isolation and physiological, molecular, and cellular experiments. J.C., B.N.F., B.H.C, and N.O.D. interpreted data and edited the manuscript. R.J.K. supported the study.

CREDIT AUTHORSHIP CONTRIBUTION STATEMENT

Zhouji Chen: Writing — review & editing, Writing — original draft, Validation, Supervision, Project administration, Methodology, Investigation, Formal analysis, Data curation, Conceptualization. **Shiyu Wang:** Writing — review & editing, Validation, Methodology, Investigation, Formal analysis, Data curation, Conceptualization. **Anita Pottekat:** Writing — review & editing, Validation, Methodology, Investigation. **Alec Duffey:** Writing — review & editing, Methodology, Investigation, Data curation. **Insook Jang:** Writing — review & editing, Methodology, Investigation. **Benny H. Chang:** Writing — review & editing, Resources, Methodology. **Jaehyung Cho:** Writing — review & editing, Resources, Methodology. **Brian N. Finck:** Writing — review & editing, Resources, Methodology. **Nicholas O. Davidson:** Writing — review & editing, Resources, Methodology. **Randal J. Kaufman:** Writing — review & editing, Supervision, Resources, Project administration, Investigation, Funding acquisition, Formal analysis, Data curation, Conceptualization.

ACKNOWLEDGEMENTS

We thank the UCSD EM and microscopy cores, the SBP Histology lab. Portions of this work were supported by NIH Grants DK103185, CA198103, DK113171, and P01HL160472 (To R.J.K.), and R01 DK117657 (To B.N.F), and DK52574, DK119437, and HL151328 (To N.O.D).

DECLARATION OF COMPETING INTEREST

There is no conflict of interest to be declared.

DATA AVAILABILITY

Data will be made available on request.

APPENDIX A. SUPPLEMENTARY DATA

Supplementary data to this article can be found online at https://doi.org/10.1016/j.molmet.2024.101874.

REFERENCES

[1] Bamba V, Rader DJ. Obesity and atherogenic dyslipidemia. Gastroenterology 2007;132:2181–90.

[2] Chait A, Ginsberg HN, Vaisar T, Heinecke JW, Goldberg IJ, Bornfeldt KE. Remnants of the triglyceride-rich lipoproteins, diabetes, and cardiovascular disease. Diabetes 2020;69:508–16.

[3] Sniderman AD, Thanassoulis G, Glavinovic T, Navar AM, Pencina M, Catapano A, et al. Apolipoprotein B particles and cardiovascular disease: a narrative review. JAMA Cardiol 2019;4:1287–95.

[4] Heeren J, Scheja L. Metabolic-associated fatty liver disease and lipoprotein metabolism. Mol Metabol 2021;50:101238.

[5] Adiels M, Olofsson SO, Taskinen MR, Boren J. Overproduction of very low-density lipoproteins is the hallmark of the dyslipidemia in the metabolic syndrome. Arterioscler Thromb Vasc Biol 2008;28:1225–36.

[6] Sundaram M, Yao Z. Recent progress in understanding protein and lipid factors affecting hepatic VLDL assembly and secretion. Nutr Metab 2010;7:35.

[7] Sirwi A, Hussain MM. Lipid transfer proteins in the assembly of apoB-containing lipoproteins. J Lipid Res 2018;59:1094–102.

[8] Schonfeld G, Patterson BW, Yablonskiy DA, Tanoli TS, Averna M, Elias N, et al. Fatty liver in familial hypobetalipoproteinemia: triglyceride assembly into VLDL particles is affected by the extent of hepatic steatosis. J Lipid Res 2003;44:470–8.

[9] Sookoian S, Pirola CJ, Valenti L, Davidson NO. Genetic pathways in nonalcoholic fatty liver disease: insights from systems biology. Hepatology 2020;72:330–46.

[10] Duran EK, Pradhan AD. Triglyceride-rich lipoprotein remnants and cardiovascular disease. Clin Chem 2021;67:183–96.

[11] Chen Z, Fitzgerald RL, Averna MR, Schonfeld G. A targeted apolipoprotein B-38.9-producing mutation causes fatty livers in mice due to the reduced ability of apolipoprotein B-38.9 to transport triglycerides. J Biol Chem 2000;275:32807–15.

[12] Chen Z, Fitzgerald RL, Schonfeld G. Hypobetalipoproteinemic mice with a targeted apolipoprotein (Apo) B-27.6-specifying mutation: in vivo evidence for an important role of amino acids 1254-1744 of ApoB in lipid transport and metabolism of the apoB-containing lipoprotein. J Biol Chem 2002;277:14135–45.

[13] Boren J, Adiels M, Bjornson E, Matikainen N, Soderlund S, Ramo J, et al. Effects of TM6SF2 E167K on hepatic lipid and very low-density lipoprotein metabolism in humans. JCI Insight 2020;5.

[14] Chen Z, Davidson NO. Genetic regulation of intestinal lipid transport and metabolism. In: Johnson LR, Barrett KE, Ghishan FK, Merchant JL, Said HM, Wood JD, editors. Physiology of the gastrointestinal tract. Volume 2. 5th ed. Amsterdam: Elsevier Inc.; 2012. p. 1643–62.

[15] Fujita K, Nozaki Y, Wada K, Yoneda M, Fujimoto Y, Fujitake M, et al. Dysfunctional very-low-density lipoprotein synthesis and release is a key factor in nonalcoholic steatohepatitis pathogenesis. Hepatology 2009;50:772–80.

[16] Imajo K, Yoneda M, Fujita K, Kessoku T, Tomeno W, Ogawa Y, et al. Oral choline tolerance test as a novel noninvasive method for predicting nonalcoholic steatohepatitis. J Gastroenterol 2014;49:295–304.

[17] Chen Z, Norris JY, Finck BN. Peroxisome proliferator-activated receptor-gamma coactivator-1alpha (PGC-1alpha) stimulates VLDL assembly through activation of cell death-inducing DFFA-like effector B (CideB). J Biol Chem 2010;285:25996–6004.

[18] Ye J, Li JZ, Liu Y, Li X, Yang T, Ma X, et al. Cideb, an ER- and lipid droplet-associated protein, mediates VLDL lipidation and maturation by interacting with apolipoprotein B. Cell Metabol 2009;9:177–90.

[19] Shin JY, Hernandez-Ono A, Fedotova T, Östlund C, Lee MJ, Gibeley SB, et al. Nuclear envelope-localized torsinA-LAP1 complex regulates hepatic VLDL secretion and steatosis. J Clin Invest 2019;129:4885–900.

[20] Wang X, Wang H, Xu B, Huang D, Nie C, Pu L, et al. Receptor-mediated ER export of lipoproteins controls lipid homeostasis in mice and humans. Cell Metabol 2021;33:350–366 e357.

[21] Newberry EP, Hall Z, Xie Y, Molitor EA, Bayguinov PO, Strout GW, et al. Liver-specific deletion of mouse Tm6sf2 promotes steatosis, fibrosis, and hepatocellular cancer. Hepatology 2021;74:1203–19.

[22] Doonan LM, Fisher EA, Brodsky JL. Can modulators of apolipoproteinB biogenesis serve as an alternate target for cholesterol-lowering drugs? Biochim Biophys Acta Mol Cell Biol Lipids 2018;1863:762–71.

[23] Wang S, Chen Z, Lam V, Han J, Hassler J, Finck BN, et al. IRE1α-XBP1s induces PDI expression to increase MTP activity for hepatic VLDL assembly and lipid homeostasis. Cell Metabol 2012;16:473–86.

[24] Kim CW, Addy C, Kusunoki J, Anderson NN, Deja S, Fu X, et al. Acetyl CoA carboxylase inhibition reduces hepatic steatosis but elevates plasma triglycerides in mice and humans: a bedside to bench investigation. Cell Metabol 2017;26:394–406 e396.

[25] Santos AJ, Nogueira C, Ortega-Bellido M, Malhotra V. TANGO1 and Mia2/cTAGE5 (TALI) cooperate to export bulky pre-chylomicrons/VLDLs from the endoplasmic reticulum. J Cell Biol 2016;213:343–54.

[26] Jiang X, Fulte S, Deng F, Chen S, Xie Y, Chao X, et al. Lack of VMP1 impairs hepatic lipoprotein secretion and promotes non-alcoholic steatohepatitis. J Hepatol 2022;77:619–31.

[27] Richardson PE, Manchekar M, Dashti N, Jones MK, Beigneux A, Young SG, et al. Assembly of lipoprotein particles containing apolipoprotein-B: structural model for the nascent lipoprotein particle. Biophys J 2005;88:2789–800.

[28] Alexander CA, Hamilton RL, Havel RJ. Subcellular localization of B apoprotein of plasma lipoproteins in rat liver. J Cell Biol 1976;69:241–63.

[29] Swift LL, Valyi-Nagy K, Rowland C, Harris C. Assembly of very low density lipoproteins in mouse liver: evidence of heterogeneity of particle density in the Golgi apparatus. J Lipid Res 2001;42:218–24.

[30] Tran K, Thorne-Tjomsland G, DeLong CJ, Cui Z, Shan J, Burton L, et al. Intracellular assembly of very low density lipoproteins containing apolipoprotein B100 in rat hepatoma McA-RH7777 cells. J Biol Chem 2002;277:31187–200.

[31] Sniderman AD, Cianflone K. Substrate delivery as a determinant of hepatic apoB secretion. Arterioscler Thromb 1993;13:629–36.

[32] Farese Jr RV, Ruland SL, Flynn LM, Stokowski RP, Young SG. Knockout of the mouse apolipoprotein B gene results in embryonic lethality in homozygotes and protection against diet-induced hypercholesterolemia in heterozygotes. Proc Natl Acad Sci U S A 1995;92:1774–8.

[33] Davidson NO, Shelness GS. APOLIPOPROTEIN B: mRNA editing, lipoprotein assembly, and presecretory degradation. Annu Rev Nutr 2000;20:169–93.

[34] Teng B, Burant CF, Davidson NO. Molecular cloning of an apolipoprotein B messenger RNA editing protein. Science 1993;260:1816–9.

[35] Hirano K, Young SG, Farese Jr RV, Ng J, Sande E, Warburton C, et al. Targeted disruption of the mouse apobec-1 gene abolishes apolipoprotein B mRNA editing and eliminates apolipoprotein B48. J Biol Chem 1996;271:9887–90.

[36] Blanc V, Davidson NO. Mouse and other rodent models of C to U RNA editing. Methods Mol Biol 2011;718:121–35.

[37] Fisher E, Lake E, McLeod RS. Apolipoprotein B100 quality control and the regulation of hepatic very low density lipoprotein secretion. J Biomed Res 2014;28:178–93.

[38] Wetterau JR, Aggerbeck LP, Bouma ME, Eisenberg C, Munck A, Hermier M, et al. Absence of microsomal triglyceride transfer protein in individuals with abetalipoproteinemia. Science 1992;258:999–1001.
[39] Berriot-Varoqueaux N, Aggerbeck LP, Samson-Bouma M, Wetterau JR. The role of the microsomal triglygeride transfer protein in abetalipoproteinemia. Annu Rev Nutr 2000;20:663–97.
[40] Raabe M, Véniant MM, Sullivan MA, Zlot CH, Björkegren J, Nielsen LB, et al. Analysis of the role of microsomal triglyceride transfer protein in the liver of tissue-specific knockout mice. J Clin Invest 1999;103:1287–98.
[41] Xie Y, Newberry EP, Young SG, Robine S, Hamilton RL, Wong JS, et al. Compensatory increase in hepatic lipogenesis in mice with conditional intestine-specific Mttp deficiency. J Biol Chem 2006;281:4075–86.
[42] Xie Y, Luo J, Kennedy S, Davidson NO. Conditional intestinal lipotoxicity in Apobec-1-/- Mttp-IKO mice: a survival advantage for mammalian intestinal apolipoprotein B mRNA editing. J Biol Chem 2007;282:33043–51.
[43] Liao W, Hui TY, Young SG, Davis RA. Blocking microsomal triglyceride transfer protein interferes with apoB secretion without causing retention or stress in the ER. J Lipid Res 2003;44:978–85.
[44] Kulinski A, Rustaeus S, Vance JE. Microsomal triacylglycerol transfer protein is required for lumenal accretion of triacylglycerol not associated with ApoB, as well as for ApoB lipidation. J Biol Chem 2002;277:31516–25.
[45] Benham AM. The protein disulfide isomerase family: key players in health and disease. Antioxidants Redox Signal 2012;16:781–9.
[46] Matsusaki M, Kanemura S, Kinoshita M, Lee YH, Inaba K, Okumura M. The protein disulfide isomerase family: from proteostasis to pathogenesis. Biochim Biophys Acta Gen Subj 2020;1864:129338.
[47] Jessop CE, Chakravarthi S, Watkins RH, Bulleid NJ. Oxidative protein folding in the mammalian endoplasmic reticulum. Biochem Soc Trans 2004;32:655–8.
[48] Gilbert HF. Protein disulfide isomerase and assisted protein folding. J Biol Chem 1997;272:29399–402.
[49] Jessop CE, Bulleid NJ. Glutathione directly reduces an oxidoreductase in the endoplasmic reticulum of mammalian cells. J Biol Chem 2004;279:55341–7.
[50] Araki K, Iemura S, Kamiya Y, Ron D, Kato K, Natsume T, et al. Ero1-alpha and PDIs constitute a hierarchical electron transfer network of endoplasmic reticulum oxidoreductases. J Cell Biol 2013;202:861–74.
[51] Jha V, Kumari T, Manickam V, Assar Z, Olson KL, Min JK, et al. ERO1-PDI redox signaling in health and disease. Antioxidants Redox Signal 2021;35:1093–115.
[52] Fass D, Thorpe C. Chemistry and enzymology of disulfide cross-linking in proteins. Chem Rev 2018;118:1169–98.
[53] Wang CC. Protein disulfide isomerase assists protein folding as both an isomerase and a chaperone. Ann N Y Acad Sci 1998;864:9–13.
[54] Klappa P, Ruddock LW, Darby NJ, Freedman RB. The b' domain provides the principal peptide-binding site of protein disulfide isomerase but all domains contribute to binding of misfolded proteins. EMBO J 1998;17:927–35.
[55] Puig A, Lyles MM, Noiva R, Gilbert HF. The role of the thiol/disulfide centers and peptide binding site in the chaperone and anti-chaperone activities of protein disulfide isomerase. J Biol Chem 1994;269:19128–35.
[56] Lamberg A, Jauhiainen M, Metso J, Ehnholm C, Shoulders C, Scott J, et al. The role of protein disulphide isomerase in the microsomal triacylglycerol transfer protein does not reside in its isomerase activity. Biochem J 1996;315(Pt 2):533–6.
[57] Ritchie PJ, Decout A, Amey J, Mann CJ, Read J, Rosseneu M, et al. Baculovirus expression and biochemical characterization of the human microsomal triglyceride transfer protein. Biochem J 1999;338(Pt 2):305–10.
[58] Linnik KM, Herscovitz H. Multiple molecular chaperones interact with apolipoprotein B during its maturation. The network of endoplasmic reticulum-resident chaperones (ERp72, GRP94, calreticulin, and BiP) interacts with apolipoprotein b regardless of its lipidation state. J Biol Chem 1998;273:21368–73.
[59] Wang S, Park S, Kodali VK, Han J, Yip T, Chen Z, et al. Identification of protein disulfide isomerase 1 as a key isomerase for disulfide bond formation in apolipoprotein B100. Mol Biol Cell 2015;26:594–604.
[60] Hahm E, Li J, Kim K, Huh S, Rogelj S, Cho J. Extracellular protein disulfide isomerase regulates ligand-binding activity of alphaMbeta2 integrin and neutrophil recruitment during vascular inflammation. Blood 2013;121:3789–800. S3781-3715.
[61] He K, Cunningham CN, Manickam N, Liu M, Arvan P, Tsai B. PDI reductase acts on Akita mutant proinsulin to initiate retrotranslocation along the Hrd1/Sel1L-p97 axis. Mol Biol Cell 2015;26:3413–23.
[62] Blackhart BD, Yao ZM, McCarthy BJ. An expression system for human apolipoprotein B100 in a rat hepatoma cell line. J Biol Chem 1990;265:8358–60.
[63] Hassler JR, Scheuner DL, Wang S, Han J, Kodali VK, Li P, et al. The IRE1α/XBP1s pathway is essential for the glucose response and protection of β cells. PLoS Biol 2015;13:e1002277.
[64] Chen Z, Newberry EP, Norris JY, Xie Y, Luo J, Kennedy SM, et al. ApoB100 is required for increased VLDL-triglyceride secretion by microsomal triglyceride transfer protein in ob/ob mice. J Lipid Res 2008;49:2013–22.
[65] Sampey BP, Stewart BJ, Petersen DR. Ethanol-induced modulation of hepatocellular extracellular signal-regulated kinase-1/2 activity via 4-hydroxynonenal. J Biol Chem 2007;282:1925–37.
[66] Millar JS, Cromley DA, McCoy MG, Rader DJ, Billheimer JT. Determining hepatic triglyceride production in mice: comparison of poloxamer 407 with Triton WR-1339. J Lipid Res 2005;46:2023–8.
[67] Chen Z, Fitzgerald RL, Saffitz JE, Semenkovich CF, Schonfeld G. Amino terminal 38.9% of apolipoprotein B-100 is sufficient to support cholesterol-rich lipoprotein production and atherosclerosis. Arterioscler Thromb Vasc Biol 2003;23:668–74.
[68] Xie Y, Fung HY, Newberry EP, Kennedy S, Luo J, Crooke RM, et al. Hepatic Mttp deletion reverses gallstone susceptibility in L-Fabp knockout mice. J Lipid Res 2014;55:540–8.
[69] Chang BH, Liao W, Li L, Nakamuta M, Mack D, Chan L. Liver-specific inactivation of the abetalipoproteinemia gene completely abrogates very low density lipoprotein/low density lipoprotein production in a viable conditional knockout mouse. J Biol Chem 1999;274:6051–5.
[70] Rutkevich LA, Cohen-Doyle MF, Brockmeier U, Williams DB. Functional relationship between protein disulfide isomerase family members during the oxidative folding of human secretory proteins. Mol Biol Cell 2010;21:3093–105.
[71] Lin X, Schonfeld G, Yue P, Chen Z. Hepatic fatty acid synthesis is suppressed in mice with fatty livers due to targeted apolipoprotein B38.9 mutation. Arterioscler Thromb Vasc Biol 2002;22:476–82.
[72] Lin MC, Gordon D, Wetterau JR. Microsomal triglyceride transfer protein (MTP) regulation in HepG2 cells: insulin negatively regulates MTP gene expression. J Lipid Res 1995;36:1073–81.
[73] Gordon DA, Jamil H. Progress towards understanding the role of microsomal triglyceride transfer protein in apolipoprotein-B lipoprotein assembly. Biochim Biophys Acta 2000;1486:72–83.
[74] Chen Z, Gropler MC, Norris J, Lawrence Jr JC, Harris TE, Finck BN. Alterations in hepatic metabolism in fld mice reveal a role for lipin 1 in regulating VLDL-triacylglyceride secretion. Arterioscler Thromb Vasc Biol 2008;28:1738–44.
[75] Grubb S, Guo L, Fisher EA, Brodsky JL. Protein disulfide isomerases contribute differentially to the endoplasmic reticulum-associated degradation of apolipoprotein B and other substrates. Mol Biol Cell 2012;23:520–32.
[76] Hetz C, Zhang K, Kaufman RJ. Mechanisms, regulation and functions of the unfolded protein response. Nat Rev Mol Cell Biol 2020;21:421–38.

